Electrohydrodynamic Interactions of an AFM Tip and a Biological Membrane

Tai-Hsi Fan and Andrei G. Fedorov

Multiscale Integrated Thermofluidics Lab., G. W. Woodruff School of Mechanical Engineering,
Georgia Institute of Technology, Atlanta, Georgia 30332-0405, USA

ABSTRACT

We report the electrohydrodynamic force at the surface of the AFM tip and elastic deformation of the soft biological membranes induced by the AFM probing action, which are essential for quantitative interpretation the AFM images in the aqueous environment. This study is the first theoretical demonstration, that in addition to the electrical force induced by the non-uniform electric field around the AFM tip, the feedback force at the AFM tip during imaging in an aqueous environment is also due to the strong coupling of electrohydrodynamic interactions in the solution and elastic deformation of the membrane. We also show that the fluid-tip-membrane coupling dynamics is characterized by the following dimensionless numbers: the electric force parameter, the characteristic Debye length, the membrane electric potential, the relative tip-to-electrolyte dielectric constant, and elastic properties of the membrane.

Keyworlds: AFM, Electrohydrodynamics, Biomembranes

1 INTRODUCTION

Atomic Force Microscopy (AFM) provides unique opportunities to investigate the structure, morphology, micromechanical properties, and biochemical signaling activity of cells, subcell structures, and even single molecules with high temporal and spatial resolutions [1]. In biological applications, AFM imaging needs to be performed in the natural (aqueous) living environment of the cell in order to observe molecular level interactions and biochemical processes *in-situ* in the electrolyte solution and to avoid the interference due to the capillary adhesion forces. Despite significant advances made in experimental application of AFM in cell imaging, the data interpretation and associated theoretical models are still in their infancy. This is perhaps owing to the overwhelming complexity of the physical/chemical phenomena taking place during an AFM imaging of flexible, electrochemically active biological samples, which includes intimately coupled fluid flow (inside and outside of the cell), dynamics of the cell membrane deformation, and electrodynamics of ionic interactions in the electrolyte and surface double layers. The critical importance of understanding these interactions should not be overlooked, as pointed out by Kamm in his recent review of cellular fluid mechanics [2], because of the critical role of the flow conditions on the biological functions, normal physiology and disease of living cells. In our previous work [3], the physical processes taking place during AFM imaging of soft biological membranes (Fig. 1) were investigated in detail. A particular emphasis was placed on the understanding of hydrodynamic effects in the fluid inside and outside of the cell associated with elastic deformation of the membrane in response to the AFM tapping action for the entire probing cycle. In this paper, we extend our prior work by including the electrodynamic effects on the fluid motion and surface forces to obtain an integrated electrohydrodynamic model describing the AFM tip and biomembrane interactions. The model couples the fluid flow (inside and outside of the cell membrane), ion distribution, electrical forces, membrane surface charge, and dynamics of membrane deformation.

2 THEORETICAL DEVELOPMENTS

2.1 Scaling and Model Formulation

The electrolyte is considered to be homogeneous with uniform electrical and fluid properties on both sides of the cell membrane, whose surface potential or charge density are uniform and described by a symmetric zeta potential. We also assume that the short-range van-der-Waals, hydration, and other molecular level interactions are negligible compared to the electrodynamic forces when the AFM tip penetrates into the electric double-layer of the membrane. Both the environment fluid and the fluid inside the cell are assumed incompressible Newtonian fluids with the same density and viscosity. The membrane thickness is neglected and mathematically treated as an infinitesimally thin interface. Thermal fluctuations are assumed to be negligible so that the membrane surface is

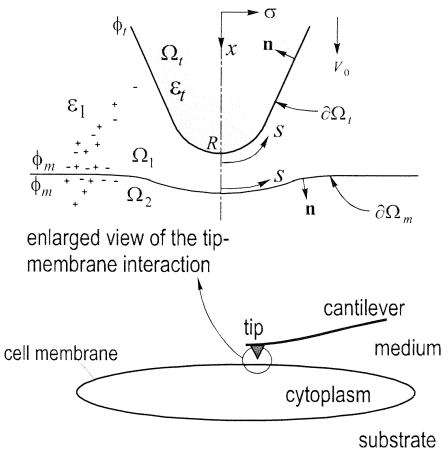

Figure 1: Schematic view of an AFM tip approaching a cell membrane and definition of the computational domain.

perfectly smooth. We do not consider the ion transport across

the cell membrane and the Lorentz electric force is the only body force involved in the probing process. The system dynamics is modeled by the electrically forced non-homogeneous Stokes equation for fluid flow, the linearized Poisson-Boltzmann equation for the electric potential distribution in the electrolyte environment, the Laplace equation for the electric potential within the dielectric AFM tip, and the Helfrich and Zhon-can's equation is used to describe the equilibrium shape of the bio-membrane. To make the results general, we render the governing equations dimensionless by using the following scales: length scale is given by the AFM tip radius R, velocity $\mathbf{u}$ is scaled by the tip approach velocity V_0, time is scaled by R/V_0, the local surface tension γ is scaled by $V_0\mu$ with μ being dynamic viscosity, the membrane bending rigidity B is scaled by $V_0\mu R^2$, the membrane mean curvature H and spontaneous curvature c_0 are both scaled by $1/R$, the Gaussian curvature K is scaled by $1/R^2$, surface force f and pressure p are scaled by $V_0\mu/R$, the electric potential ϕ is scaled by $\zeta\left(\zeta = kT/e\right)$ where k is Boltzmann constant, T is an absolute temperature, and e is the single electron charge. Using these scales, the dimensionless governing equations for the electric field potential and electrohydrodynamic stress are:

(i) Linearized Poisson-Boltzmann and Laplace equations [4]:

$$\nabla^2\phi = (\kappa R)^2\phi\,,\quad \mathbf{x}\in\Omega_1+\Omega_2 \tag{1}$$

$$\nabla^2\phi = 0\,,\quad \mathbf{x}\in\Omega_t \tag{2}$$

(ii) Quasi-steady, electrically forced Stokes equation and the continuity equation with combined hydrodynamic and Maxwell electric stresses [5]:

$$\nabla\cdot\left(\boldsymbol{\tau}^h+\boldsymbol{\tau}^e\right) = -\nabla p+\nabla^2\mathbf{u}+\alpha\phi\nabla\phi = 0\,,\quad \mathbf{x}\in\Omega_1+\Omega_2 \tag{3}$$

$$\nabla\cdot\mathbf{u} = 0\,,\quad \mathbf{x}\in\Omega_1+\Omega_2 \tag{4}$$

where $\mathbf{x}$ denotes a position vector in the Cartesian coordinate system, and the volumetric charge density has been linearized about the equilibrium ion distribution. The Maxwell stress tensor and the electric field can be written in dimensionless form as

$$\boldsymbol{\tau}^e = \omega\left(\frac{\partial\phi}{\partial x_i}\frac{\partial\phi}{\partial x_j}-\frac{1}{2}\frac{\partial\phi}{\partial x_k}\frac{\partial\phi}{\partial x_k}\delta_{ij}\right)\,,\quad \mathbf{E} = -\frac{\zeta}{R}\nabla\phi \tag{5}$$

with the term in front of the Kronecker delta δ_{ij} denoting the isotropic stress component.

(iii) Dynamic boundary condition at the membrane interface is given by the Landau's general dynamic interface model [6] combined with Helfrich membrane mechanics and Zhong-can's equilibrium shape equation [7,8], in terms of normal and shear components of the total (hydrodynamic and electric) stress tensor as described in detail in [3],

$$\begin{aligned}&(\boldsymbol{\tau}_2\cdot\mathbf{n}-\boldsymbol{\tau}_1\cdot\mathbf{n})\cdot\mathbf{n} = -2\gamma H+\\ &B(2H+c_0)(2H^2-2K-c_0H)+2B\nabla^2H\end{aligned} \tag{6}$$

$$(\boldsymbol{\tau}_2\cdot\mathbf{n}-\boldsymbol{\tau}_1\cdot\mathbf{n})\cdot\mathbf{t} = \nabla_s\gamma \tag{7}$$

(iv) Finally, the formulation is completed by introducing the local area constraint condition $\partial(dA)/\partial t = 0$ [3] in order to find an unknown tension/compression force γ due to the surface force jump given by Eqs. (6) and (7).

Dimensionless parameters in Eqs. (1, 3, 5) are the electric force and electric stress parameters α and ω, respectively, both scaled by the viscous force $V_0\mu/R$, and the characteristic diffusion length κR of the electric double layer based on the Debye length κ^{-1}:

$$\alpha = \frac{\varepsilon\varepsilon_0\kappa^2R\zeta^2}{\mu V_0}\,,\quad \omega = \frac{\varepsilon\varepsilon_0\zeta^2}{\mu V_0R}\,,\quad \kappa = \sqrt{\frac{e^2}{\varepsilon\varepsilon_0kT}\sum_i\left(z_i^2n_i^\infty\right)} \tag{8}$$

where ε is the relative electric permittivity, ε_0 is the permittivity of the vacuum, and the summation term inside the expression for Debye length κ represents the ionic strength of the electrolyte solution with z_i and n_i^∞ being, respectively, the valence number and the bulk concentration for each ionic species i. The system of governing equations (1-7) is complemented by the boundary conditions:

$$\begin{aligned}&\mathbf{u}(\mathbf{x}) = 1\,\hat{\mathbf{e}}_x\,,\ \mathbf{x}\in\partial\Omega_t\,;\quad \mathbf{u}(\mathbf{x}) = \mathbf{u}_m(\mathbf{x})\,,\ \mathbf{x}\in\partial\Omega_m\,;\\ &\mathbf{u}(\mathbf{x}) = 0\,,\quad \mathbf{x}\to\infty\,;\\ &\phi_1(\mathbf{x}) = \phi_2(\mathbf{x}) = \phi_m\,,\quad \mathbf{x}\in\partial\Omega_m \text{ toward } \Omega_1 \text{ and } \Omega_2\,;\\ &\phi(\mathbf{x}) = 0\,,\quad \mathbf{x}\to\infty\,;\quad \phi_1(\mathbf{x}) = \phi_t(\mathbf{x})\,,\quad \mathbf{x}\in\partial\Omega_t\,;\\ &\varepsilon_r\nabla\phi_t(\mathbf{x})\cdot\mathbf{n}(\mathbf{x}) = \nabla\phi_1(\mathbf{x})\cdot\mathbf{n}(\mathbf{x})\,,\ \mathbf{x}\in\partial\Omega_t\end{aligned} \tag{9}$$

where the relative dielectric constant is defined by $\varepsilon_r = \varepsilon_t/\varepsilon_1$. Several assumptions are made in the boundary conditions to simplify problem: (i) the AFM tip approach speed remains constant during imaging process, (ii) the membrane electric potential is small, $|\phi| << \zeta$, so that the Poisson-Boltzmann equation can be linearized, (iii) the polar groups of the lipid molecules keep the electric potential unifom across the membrane, (iv) the AFM tip has zero surface charge density.

2.2 Boundary Integral Formulation

The model equations are intimately coupled and solved by the boundary integral method. According to Ladyzhenskaya [9], the integral form of the dimensionless, nonhomogeneous Stokes equation combines the contributions from *Stokeslet, Stresslet,* and nonhomogeneous source terms and is given by:

$$\begin{aligned}\lambda u_j(\mathbf{x}_0) = &-\int_\Omega S_i(\mathbf{x})G_{ij}(\mathbf{x},\mathbf{x}_0)\,dV(\mathbf{x})\\ &-\int_{\partial\Omega}\tau_{ik}(\mathbf{x})n_k(\mathbf{x})G_{ij}(\mathbf{x},\mathbf{x}_0)\,dA(\mathbf{x})\\ &+\overset{p.v.,\,\mathbf{x}_0\in\partial\Omega}{\int_{\partial\Omega}}u_i(\mathbf{x})T_{ijk}(\mathbf{x},\mathbf{x}_0)n_k(\mathbf{x})dA(\mathbf{x})\end{aligned} \tag{10}$$

where $\lambda=0$ for $\mathbf{x}_0 \notin \Omega$, $\lambda=8\pi$ for $\mathbf{x}_0 \in \Omega-\partial\Omega$, and $\lambda=4\pi$ for $\mathbf{x}_0 \in \partial\Omega$. Also, the unit surface normal vector n_j points into the fluid domain, S_i represents the vector source term due to Lorentz electric force in Eq. (3), u_i and τ_{ik} represent the velocity and electrohydrodynamic stress fields. Note that when the source point is located at the boundary, $\mathbf{x}_0 \in \partial\Omega$, the double layer Stresslet contribution has to be interpreted in the sense of Cauchy principal value because of the stronger singularity in the integral kernel T_{ijk}. The fundamental solution (*Stokeslet*) and its corresponding stress field (*Stresslet*) are given by [10],

$$G_{ij}(\mathbf{x},\mathbf{x}_0)=\frac{\delta_{ij}}{r}+\frac{r_i r_j}{r^3}, \quad T_{ijk}(\mathbf{x},\mathbf{x}_0)=-6\frac{r_i r_j r_k}{r^5} \tag{11}$$

respectively, where δ_{ij} is the Kronecker delta function, $\mathbf{r}=\mathbf{x}\text{-}\mathbf{x}_0$ is the position vector between the field and source points, and $r=|\mathbf{x}\text{-}\mathbf{x}_0|$ is the distance between them. Further, the domain integral of the source term $S_i=-\alpha\phi\nabla\phi$ can be transformed into the surface integral by incorporating the divergence free property of the *Stokeslet*, $\nabla\cdot G_{ij}=0$, i.e,

$$\int_\Omega \phi\frac{\partial\phi}{\partial x_i}G_{ij}\,dV=\frac{1}{2}\int_\Omega \nabla\cdot\left(\phi^2 G_{ij}\right)dV \tag{12}$$

Thus, the boundary integral formulation of Eq. (3) becomes

$$\begin{aligned}\lambda u_j &= -\frac{\alpha}{2}\int_{\partial\Omega}\phi^2 G_{ij}\,n_i\,dA \\ &- \int_{\partial\Omega}\tau_{ik}n_k G_{ij}\,dA+\int_{\partial\Omega}u_i T_{ijk}\,n_k\,dA\end{aligned} \tag{13}$$

Eq. (13) is valid for the fluids on both sides of the biomembrane, and the domains can be effectively combined leading to the following unified domain formulation [3]:

$$\begin{aligned}\lambda u_j &= -\int_{\partial\Omega_m}\Delta f_i G_{ij}\,dA \\ &+\int_{\partial\Omega_t}\left(f_i+\frac{\alpha}{2}\phi_t^2 n_i\right)G_{ij}dA-\int_{\partial\Omega_t}^{p.v.,\,\mathbf{x}_0\in\partial\Omega_t}u_i T_{ijk}n_k dA\end{aligned} \tag{14}$$

where $\lambda=8\pi$ for $\mathbf{x}_0\in\Omega_1+\Omega_2+\partial\Omega_m$, and $\lambda=4\pi$ for $\mathbf{x}_0\in\partial\Omega_t$. Note that the traction term is replaced by the surface force $f_i=\tau_{ik}n_k$ for convenience, and the surface force jump condition $\Delta f_i=f_i^{(2)}-f_i^{(1)}$ in the kernel function can be interpreted as the source density acting on the fluid from the cell membrane surface. Clearly, the solution of linearized Poisson-Boltzmann and Laplace equations, Eqs. (1) and (2), can also be expressed in terms of integral equations:

$$\lambda_1\phi_1=\int_{\partial\Omega}\left(G_{PB}\frac{\partial\phi_1}{\partial n}-\phi_1\frac{\partial G_{PB}}{\partial n}\right)dA, \tag{15}$$

$$\lambda_t\phi_t=\int_{\partial\Omega}\left(G_L\frac{\partial\phi_t}{\partial n}-\phi_t\frac{\partial G_L}{\partial n}\right)dA \tag{16}$$

respectively, where $\lambda_1=0.5$ for $\mathbf{x}_0\in\partial\Omega_t+\partial\Omega_m$, $\lambda_1=1.0$ for $\mathbf{x}_0\in\Omega_1$, $\lambda_t=0.5$ for $\mathbf{x}_0\in\partial\Omega_t$, and $\lambda_t=1.0$ for $\mathbf{x}_0\in\Omega_t$. Note that the coefficient value 0.5 is for the smooth boundary. And the fundamental solutions are given by

$$G_{PB}=e^{-(\kappa R)r}/4\pi r, \quad G_L=1/4\pi r \tag{17}$$

As shown in Fig. (1), the AFM tip and cell membrane are axisymmetric, so the complexity of the integral formulations can be further reduced by using the cylindrical coordinate system and expressing the fundamental solutions in terms of the Green's functions of the ring source type. Finally, the membrane constraint equation can be expressed in terms of the arc-length with the local surface tangent $\hat{\mathbf{t}}(\mathbf{x}\in\partial\Omega_m)$ [3]:

$$\sigma\left(\frac{\partial u_x}{\partial s}\hat{\mathbf{t}}_x+\frac{\partial u_\sigma}{\partial s}\hat{\mathbf{t}}_\sigma\right)+u_\sigma=0, \quad \mathbf{x}_0\in\partial\Omega_m \tag{18}$$

In the final form, the complex three-dimensional system of integral equations for the coupled electric field/fluid flow/membrane deformation problem, described by Eqs. (14-16, 18) and boundary conditions Eqs. (6,7,9), is reduced to one-dimensional form using axisymmetric integral representation and is solved numerically using the boundary element method with discretization along the surface of the AFM tip and the cell membrane [3]. Due to the limited space, the details of all transformations are not shown, but will be reported in the follow-up publications.

2.3 AFM Feedback Force

The total force acting on the AFM tip is due to: (i) the electrohydrodynamic stress owing to the electrically (Lorentz force) driven fluid motion, and (ii) the Maxwell stress generated by the electric field in the vicinity of the AFM tip induced by the charged biomembrane. The first part is obtained by direct integration of the integral solution f_i of Eq. (14) along the surface boundary of the AFM tip,

$$\mathbf{F}_{tip}^{eh}=2\pi\int_{\partial\Omega_t}\sigma\,f_i\,d\ell \tag{19}$$

and the second part, contributed by Maxwell stress, is obtained by surface integration of the solution ϕ_1 of Eq. (15),

$$\mathbf{F}_{tip}^{M}=2\pi\omega\int_{\partial\Omega_t}\sigma\frac{\partial\phi}{\partial x}\frac{\partial\phi}{\partial n}-\frac{\sigma}{2}\left[\left(\frac{\partial\phi}{\partial x}\right)^2+\left(\frac{\partial\phi}{\partial\sigma}\right)^2\right]n_x\,d\ell \tag{20}$$

RESULTS AND DISCUSSION

The Maxwell stress contribution to the force acting at the AFM tip, given by Eq. (20), has been studied before, see for example [11]. Here we only demonstrate the electrohydrodynamic effects

by considering three basic interaction processes in respect to direction of the tip movement to characterize the fundamental modes of tip-membrane interactions: first, the AFM tip approaches an initially horizontal membrane with a constant velocity in positive x direction (*forward*); second, the tip returns to its initial position moving in negative x direction (*reverse*); and third, the tip stops at its upper state and the membrane is allowed to freely relax and slowly return to its undeformed horizontal state (*relaxation*). Three typical cases A to C with increasing ionic strength of the electrolyte solution are examined and compared to the purely hydrodynamic case D. The results are shown in terms of the AFM force-distance curve for the tip with 60° opening angle, constant tip approach speed, the membrane bending rigidity $B = 1.0$, and the relative dielectric constant $\varepsilon_r = 0.075$. The test conditions are listed below:

A	B	C	D
$R = 50\,nm$	$15\,nm$	$5\,nm$	$50\,nm$
$\kappa^{-1} = 96\,nm$	$30.4\,nm$	$9.6\,nm$	∞
$n_c^{\infty} = 10^{-5} M$	$10^{-4} M$	$10^{-3} M$	0
$\kappa R = 0.52$	0.493	0.52	0
$\alpha = 160$	479	1601	0
$\omega = 590$	1968	5903	0
$\phi_m = \pm 0.25$	± 0.5	± 0.5	0
$(V_0 = 10^{-5}\ m/s,\ \mu = 1.5 \times 10^{-3}\ kg/m/s, \varepsilon_1 = 80)$			

where n_c^{∞} is a representative ionic strength with 1:1 electrolyte concentration. Figure 2 compares the force vs. tip-to-membrane separation curves for the purely hydrodynamic system [3] and when Lorentz force contribution is taken into account. The results show that the homogeneous Stokes system (i.e., case D with no Lorentz force) can be a good approximation for the system A owing to its low ionic strength. At higher ionic strength (system B) the Lorentz force contribution increases as the AFM tip approaches the electric double layer of the membrane (i.e., smaller tip-to-membrane distances), and it becomes significant when the AFM tip is penetrating into the double layer. For the system C the strong ionic effect exists for an entire probing cycle (i.e., in the near and far fields) because of the very large ionic strength of the electrolyte solution. In the cases B and C, even in the reverse motion of the AFM tip, the repulsive electric force overcomes an attractive hydrodynamic force and dominates the system dynamics. Also, as the ionic strength increases, the strong screening effect confines the electric double layer into a small region near the membrane and the system can be practically separated into two distinctly different domains. Outside of the double layer, the AFM tip is controlled by the purely hydrodynamic attractive forces well described by the homogeneous Stokes system; whereas when the AFM tip penetrates into the thin double layer, the feedback force is dominated by the strongly repuslive osmotic pressure forces and the viscous fluid forces can be neglected. Analysis of governing equations and numerical tests show that the feedback force acting at the AFM tip is mainly controlled by (i) the two correlated dimensionless parameters, α and κR, (ii) the separation distance between an AFM tip and membrane relative to the double layer thickness, and (iii) the membrane surface charge and the material dielectric constants. When Maxwell stress is accounted for, one more dimensionless parameter ω needs to be considered to assess contribution of the Maxwell stress relative for Lorentz and hydrodynamic viscous forces.

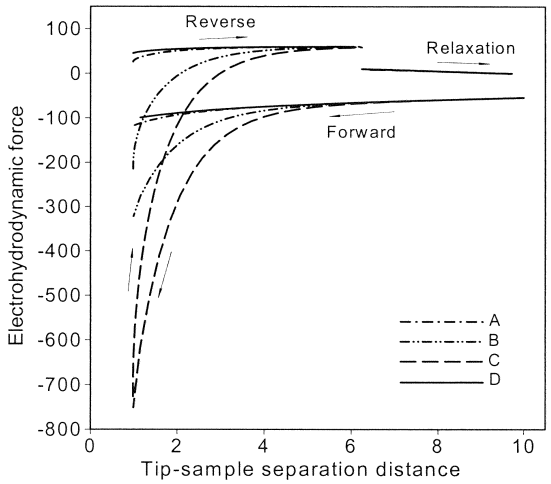

Figure 2: Electrohydrodynamic force (scaled by $V_0 \mu R$) vs. tip-membrane separation distance (scaled by R) in a full probing cycle for varying ionic strength of the electrolyte.

CONCLUSIONS

A theoretical model has been developed to reveal the relative contributions of the electric Lorentz and hydrodynamic viscous forces to the feedback force acting on the dielectric AFM tip during tapping mode imaging of biomembrane in the electrolyte solution. The proposed theoretical methodology provides new insight and quantitative information that cannot be directly measured during the AFM experiment, but essential for interpretation of the imaging data.

REFERENCES

[1] Lal, R. and John, S.A. (1994), Am.J. Physiol. **266**, C1-C21.
[2] Kamm, R.D. (2002), Annu. Rev. Fluid Mech. **34**, 211-232.
[3] Fan, T.H. and Fedorov, A.G. (2002), Langmuir (in review).
[4] Israelachvili, J.N. (1998), *Intermolecular and surface forces,* Academic Press, San Diego.
[5] Melcher, J.R. and Taylor, G.I. (1969), Annu. Rev. Fluid Mech. **1**, 111-146.
[6] Landau, L.D. & Lifshitz, E.M. (1959), *Fluid Mechanics*, Pergamon Press, London.
[7] Helfrich, W. (1973) Z. Naturforsch. Teil C **28**, 693.
[8] Ou-Yang Zhong-can (2001), Thin Solid Films **393**, 19-23.
[9] Ladyzhenskya, O.A. (1969), *The mathematical theory of viscous incompressible flow*, Gordon & Breach, New York.
[10] Pozrikidis, C. (1992), *Boundary integral and singularity methods for linearized viscous flow,* Cambridge University Press, Cambridge.
[11] Butt, H.-J. (1992), Nanotechnology **3**, 60-68.